



Contents lists available at ScienceDirect

## Journal of Non-Crystalline Solids

journal homepage: [www.elsevier.com/locate/jnoncrysol](http://www.elsevier.com/locate/jnoncrysol)

# Inelastic neutron and low-frequency Raman scattering in a niobium-phosphate glass for Raman gain applications

T. Unruh<sup>a,b</sup>, A. Schulte<sup>c,\*</sup>, Y. Guo<sup>c</sup>, W. Schirmacher<sup>b,d,\*</sup>, B. Schmid<sup>d</sup>

<sup>a</sup> Neutronenquelle "Heinz Maier-Leibnitz" (FRM II), Technische Universität München, D-85747, Garching, Germany

<sup>b</sup> Physik-Department E13, Technische Universität München, D-85747 Garching, Germany

<sup>c</sup> Department of Physics and College of Optics and Photonics, University of Central Florida, Orlando, FL 32816, USA

<sup>d</sup> Institut für Physik, Universität Mainz, D-55099 Mainz, Germany

## ARTICLE INFO

Available online xxx

## Keywords:

Raman scattering;  
Neutron scattering;  
Raman gain;  
Boson peak

## ABSTRACT

We present measurements of the vibrational spectrum of a binary niobium-phosphate glass in the THz frequency range using inelastic neutron and Raman scattering. The spectra of these glasses show a low-frequency enhancement of the vibrational density of states ("boson peak"). Using a recently developed theory of vibrational excitations in disordered solids we are able to reconcile the measured neutron and Raman spectra using fluctuating elastic and Pockels constants as a model concept. As the spontaneous Raman susceptibility is a key parameter for Raman amplification our results suggest a significant gain profile for application of niobium-phosphate glasses in Raman amplifiers.

© 2010 Elsevier B.V. All rights reserved.

## 1. Introduction

The structural disorder of glasses leads to a spectral enhancement in the 1-THz (or  $100\text{ cm}^{-1}$ ) regime, which shows up both in inelastic neutron and Raman spectra. This enhancement, together with a strong light-strain (Pockels) coupling leads to a rather large Raman susceptibility in the class of niobium-phosphate glasses, which make them good candidates for Raman amplifier materials. Both the enhancements of the Raman as well as the neutron spectra have been termed "boson peak", as the temperature dependence is just given by the boson function  $n(\omega) + 1 = 1/(1 - e^{-\hbar\omega/k_B T})$ . In reality this just demonstrates via the fluctuation-dissipation theorem that the underlying spectrum is temperature independent, i.e. the phenomenon is a harmonic one.

Concerning the boson peak an extended literature exists, in which the nature of the vibrational state in this frequency regime is investigated by experimental and simulational work, as well as by theoretical modelling [1–4]. However the light-vibrational coupling was hitherto discussed in terms of a phenomenological frequency-dependent function  $C(\omega)$ , and it was assumed that this function entered the prefactor of the Shuker–Gammon formula [5,6]

$$I(\omega) = [n(\omega) + 1]C(\omega)\frac{g(\omega)}{\omega}, \quad (1)$$

where  $g(\omega)$  is the vibrational density of states (DOS). As the function  $C(\omega)$  was unknown, researchers tried to determine it by comparing

\* Corresponding authors. W. Schirmacher is to be contacted at Physik-Department E13, Technische Universität München, D-85747, Garching, Germany.

E-mail addresses: [afs@physics.ucf.edu](mailto:afs@physics.ucf.edu) (A. Schulte), [wschirma@ph.tum.de](mailto:wschirma@ph.tum.de) (W. Schirmacher).

Raman data with DOS data, extracted from specific-heat or neutron scattering measurements [7,8]. Only very recently two of the present authors developed a theoretical model, in which the light-vibration coupling is modelled by spatially fluctuating Pockels constants, thereby allowing for the violation of the local momentum and angular-momentum selection rules [9]. The vibrational spectrum of the disordered solid was modelled by generalizing elasticity theory to allow for spatial fluctuations of the shear modulus [11–13]. This made it possible for the first time to treat inelastic X-ray, neutron and Raman scattering on the same footing. It was shown that the spectral shape of the "boson peak" seen by Raman scattering is not the same as that revealed by neutron scattering.

In the present contribution we report on a combined experimental and theoretical investigation of the low-frequency vibrational spectrum of  $40\text{ Nb}_2\text{O}_5$ – $60\text{ NaPO}_3$  glass in order to explore its properties as candidate for Raman gain material. As spectroscopic methods we used inelastic neutron scattering and Raman scattering. The material shows a Raman scattering intensity ten times higher than that of a silica glass [14]. It is therefore indeed a promising candidate for all-optical Raman gain applications. By applying the theoretical framework of [9] we show, that the neutron and Raman spectra can be reconciled with each other using a model which involves a spatially fluctuating shear modulus and spatially fluctuating Pockels coefficients. By this procedure valuable structural information concerning the statistics of these fluctuations is obtained.

## 2. Theory

We briefly review our theoretical framework. We model the disordered solid as an elastic continuum, allowing for spatial

fluctuations of the shear modulus  $G$ . The statistical properties of the fluctuations  $\Delta G(\mathbf{r}) = G(\mathbf{r}) - \langle G \rangle$  are represented by the correlation function

$$C_G(\mathbf{r}) = \langle \Delta G(\mathbf{r} + \mathbf{r}_0) \Delta G(\mathbf{r}_0) \rangle \equiv \langle \Delta G^2 \rangle e^{-\frac{1}{2} r^2 / \xi_G^2} \quad (2)$$

This can be shown [9,11–13] to lead to frequency-dependent complex sound velocities  $v_{L,T}^2(\omega) = v_{L,T,0}^2 - \Sigma_{L,T}(\omega)$ , where  $\omega = 2\pi\nu$ , and  $\Sigma_T(\omega) = \frac{1}{2} \Sigma_L(\omega) \equiv \Sigma(\omega)$  is the so-called self energy. The latter obeys the self-consistent equation (self-consistent Born approximation, SCBA)

$$\Sigma(\omega) = \gamma \int_{|\mathbf{k}| < k_D} \frac{d^3 \mathbf{k}}{(2\pi)^3} \tilde{C}_G(\mathbf{k}) [\chi_L(\mathbf{k}, \omega) + \chi_T(\mathbf{k}, \omega)] \quad (3)$$

where we have put  $C_G(k) = f_G \tilde{C}_G(k)$  with  $\frac{1}{8\pi^2} \int_{|\mathbf{k}| < k_D} d^3 \mathbf{k} \tilde{C}_G(\mathbf{k}) = 1$  and  $\gamma \propto f_G \langle \Delta G^2 \rangle$ . The longitudinal and transverse strain susceptibilities  $\chi_{L,T}$  are

$$\chi_{L,T}(\mathbf{k}, \omega) = k^2 G_{L,T}(\mathbf{k}, \omega) = \frac{k^2}{-\omega^2 + k^2 [v_{L,T}^2(\omega)]} \quad (4)$$

The DOS is given by

$$g(\omega) = \frac{2\omega}{3\pi} \int_{|\mathbf{k}| < k_D} \frac{d^3 \mathbf{k}}{(2\pi)^3} \text{Im}\{G_L(\mathbf{k}, \omega) + 2G_T(\mathbf{k}, \omega)\} \quad (5)$$

For the description of the light-vibration coupling the dielectric tensor is expanded with respect to the strain tensor  $u_{ij} = (1/2)[\partial_i u_j + \partial_j u_i]$  as  $\Delta \epsilon_{ij}(\mathbf{r}, t) = a_1(\mathbf{r}) \sum_l u_{ll}(\mathbf{r}, t) \delta_{ij} + a_2(\mathbf{r}) v_{ij}(\mathbf{r}, t)$  with  $v_{ij} = u_{ij} - (1/3) \delta_{ij} \sum_l u_{ll}$  [15].  $a_i$  are the opto-elastic or Pockels constants. They are now assumed [16] to have disorder-induced fluctuations  $a_{1,2}(\mathbf{r}) = a_{1,2}^{(0)} + \Delta a_{1,2}(\mathbf{r})$  with correlation functions  $C_{1,2}(\mathbf{r}) = \langle \Delta a_{1,2}(\mathbf{r}_0 + \mathbf{r}) \Delta a_{1,2}(\mathbf{r}_0) \rangle$ . The constant (average) terms  $a_{i,2}^{(0)}$  produce the usual formulae for Brillouin scattering and Raman scattering. From the fluctuating terms one obtains

$$I_{VH}(\omega) = [n(\omega) + 1] \frac{\alpha}{15} \left( \chi_{2,L}(\omega) + \frac{3}{2} \chi_{2,T}(\omega) \right) \quad (6)$$

$$I_{VV}(\omega) = \frac{4}{3} I_{VH}(\omega) + \alpha [n(\omega) + 1] \chi_{1,L}(\omega)$$

with the partial Raman susceptibilities ( $i = 1, 2$ )

$$\chi_{i,L,T}(\omega) = \text{Im} \left\{ \int \frac{d^3 \mathbf{k}}{(2\pi)^3} C_i(\mathbf{k}) \chi_{L,T}(\mathbf{k}, \omega) \right\} \quad (7)$$

where  $\alpha$  is a proportionality constant which involves the incident intensity, divided by the 4th power of the wavelength of the scattered light [9]. We assume that the Pockels correlation functions are of Gaussian form (Eq. (2)) and introduce correlation lengths  $\xi_i$  and prefactors  $f_i$  as  $C_i(k) = f_i \tilde{C}_i(k)$  with  $\frac{1}{8\pi^2} \int_{|\mathbf{k}| < k_D} d^3 \mathbf{k} \tilde{C}_i(k) = 1$ .

### 3. Inelastic neutron and Raman scattering

The  $40\text{Nb}_2\text{O}_5\text{-}60\text{NaPO}_3$  glass was prepared according to the procedure described in Ref. [18]. For neutron scattering experiments the samples powder form was filled in Nb double-cylinders with 0.1 mm wall thickness.

Inelastic neutron scattering experiment were carried out with the multi chopper time-of-flight spectrometer (TOFTOF) of the FRM II in Garching [10]. The direct geometry spectrometer is fed with neutrons of the cold source of the reactor which is operated with liquid  $\text{D}_2$  at about 25 K. The neutrons are guided to the primary part of the spectrometer by an s-shaped curved neutron guide serving as gamma

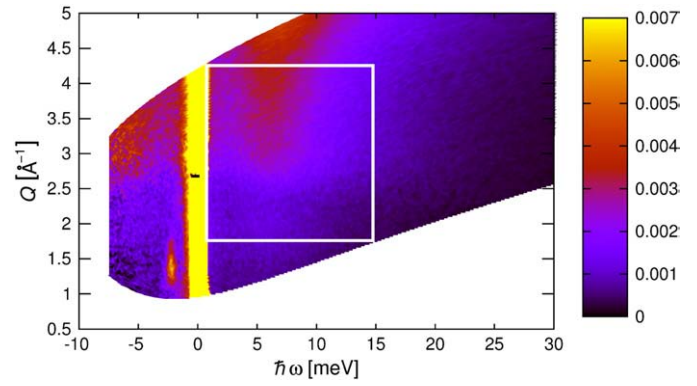


Fig. 1. Color plot of the scattering function  $S(Q, \omega)$  of  $40\text{Nb}_2\text{O}_5\text{-}60\text{NaPO}_4$  as measured by INS at the TOFTOF spectrometer. The boson peak is clearly visible on both the Stokes and the anti-Stokes side. For the calculation of the reduced DOS the region marked by the white rectangle was averaged with respect to  $Q$  (cf. text). (For interpretation of the references to color in this figure legend, the reader is referred to the web version of this article.)

ray dump and wavelength filter with a cutting edge of 1.38 Å. Using a system of 7 rotating high speed chopper discs a pulsed monochromatic beam is extracted in the primary spectrometer and focused to the sample position. The time-of-flight the neutrons scattered by the sample need to travel to the detector is measured. Corresponding time-of-flight (*tof*) spectra are collected for all of the 600 individual detectors with an effective area of about  $3 \text{ cm} \times 40 \text{ cm}$  each. The detectors are arranged at 4 m distance from the sample tangentially to the intersection line of the Debye–Scherrer cones and a virtual sphere of 4 m radius around the sample position. Thus each detector collects a *tof*-spectrum at a well defined scattering angle  $2\theta$  despite its extended length.

From the intensity measured as a function of  $2\theta$  and *tof* the calculation of the scattering function weighted by the scattering lengths of the atoms of the sample  $S(Q, \omega)$  can easily be evaluated. For this procedure the program ‘ida’ available at the spectrometer was used. The data was corrected for detector efficiencies using the elastic intensity of a vanadium measurement but also by taking the wavelength dependent sensitivity of the detectors and absorption of relevant spectrometer components into account. The data was furthermore corrected for background by subtraction of the empty can scattering. The density of states was obtained by an iterative procedure after correcting for the Debye–Waller factor and multi-phonon contributions.

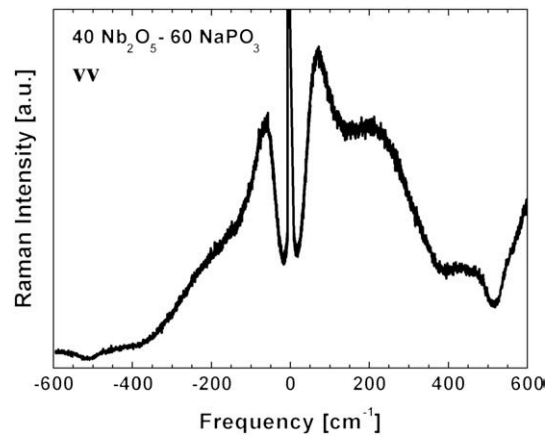
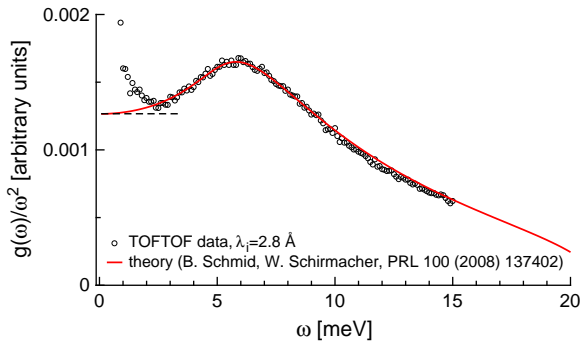


Fig. 2. Raman spectrum of  $40\text{Nb}_2\text{O}_5\text{-}60\text{NaPO}_3$  glass excited at a wavelength of 514.5 nm. Shown is the vv polarized spectrum on both the Stokes (positive frequencies) and anti-Stokes sides.



**Fig. 3.** Reduced DOS  $g(\omega)/\omega^2$  as extracted from the neutron data, compared with the corresponding result of the fluctuating-elasticity model with  $k_D v_{T,0} = 18.4$  meV/h,  $v_{L,0}/v_{T,0} = 1.7$ ,  $\gamma = 0.66\gamma_c$  with  $\gamma_c = 0.20$ . The Debye level corresponds to the onset of the calculated curve and is indicated by the dashed line. For the correlation function of the fluctuating shear modulus it was enough to treat it as a constant in the  $k$  integration regime, i.e.  $C_G(k) = C_G$ .

The constituents of our material are all coherent scatterers of similar cross section. By averaging over the full accessible scattering angle (wave vector) range we obtain a  $g(\omega)$  which gives an approximate spectral distribution of the vibrational modes [17].

In Fig. 1 a color plot of the scattering function  $S(Q, \omega)$  of  $40\text{Nb}_2\text{O}_5\text{--}60\text{NaPO}_4$  is displayed. The data were collected at the TOFTOF spectrometer [10] using 2.8 Å incident neutrons and a chopper angular frequency of 12000 rpm. This setup results in an instrumental resolution of about 500 μeV (full width at half maximum of the elastic line). The scattering function was averaged with respect to  $Q$  inside the area marked by the white rectangle in Fig. 1 to obtain an estimate for  $g(\omega)/\omega^2$ . The resulting curve is displayed in Fig. 3.

The spontaneous Raman spectra were measured in a  $\nu\nu$  geometry using 514.53 nm excitation and a double monochromator equipped with a photon counting system [18]. In Fig. 2 the measured intensity of the  $\nu\nu$  spectrum is shown on both the Stokes and anti-Stokes sides. These data have then been divided by  $\nu[n(\nu) + 1]$  to obtain the “reduced intensity”, which is depicted in Fig. 4.

#### 4. Model calculations and discussion

We found that both the neutron spectra as well as the Raman spectra could be described with short-ranged correlation functions. In order to reduce the number of free parameters we took the limit  $\xi_G, \xi_1, \xi_2 \rightarrow 0$ , i.e. the fluctuation of the shear modulus is assumed to be uncorrelated over the relevant length scales, and the same is assumed to hold for the fluctuation of the Pockels constants. This leads to  $\tilde{C}_G(k) = \tilde{C}_1(k) = \tilde{C}_2(k) = \text{const.}$  in the range of  $k \leq k_D$ . For the prefactors

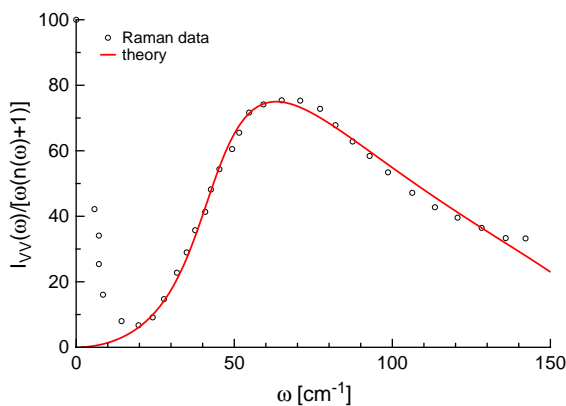


**Fig. 4.** Reduced VV Raman intensity compared with theory using the same parameters as in Fig. 3. For the correlation of the Pockels constant it was again sufficient to use  $C_1(k) = C_2(k) = \text{const.}$

of the correlation functions we used  $f_1 = f_2$ . The ratio of the sound velocity (which does not enter crucially into the calculations) was taken to have a value typical for network glasses, namely  $v_L/v_T = 1.8$ . For the disorder parameter we obtained the best fit for  $\gamma = 0.13$ , which is much smaller than the critical value  $\gamma_c = 0.20$  at which the system becomes unstable [11,12]. We note that the experimental data in Figs. 3 and 4 nicely agree with the theoretical curves, although the shapes of the spectra are quite different. This is due to the different form factors entering the DOS, Eq. (5) and the Raman intensity, Eq. (6). As noted in the Introduction previous interpretations of this discrepancy relied on the phenomenological function  $C(\omega)$ .

#### 5. Conclusions

We have shown by comparing inelastic neutron and low-frequency Raman scattering data on a  $40\text{Nb}_2\text{O}_5\text{--}60\text{NaPO}_3$  glass, candidate for all-optical Raman gain, that the vibrational spectra can be reconciled with each other and explained in terms of a model in which the structural disorder is supposed to lead to spatial fluctuations of the shear modulus and the opto-elastic (Pockels) coefficients. From our analysis it follows that the promising properties of the niobium-phosphate glass emerge from the presence of a strong transverse coupling between the dielectric and the strain tensor.

#### Acknowledgments

We thank T. Cardinal for help with the sample preparation. This work was supported in part by NSF grants ECS-0123484 and DMR-0421253 and by the Neutronenquelle “Heinz Maier-Leibnitz” (FRM II) through the allocation of beam time. A.S and W.S gratefully acknowledge travel support through the BaCaTec program.

#### References

- [1] K. Binder, W. Kob, Glassy Materials and Disordered Solids, World Scientific, Singapore, 2005.
- [2] J. Horbach, et al., Eur. Phys. J. B 19 (2001) 531.
- [3] T. Nakayama, Rep. Prog. Phys. 65 (2002) 1195.
- [4] V.L. Gurevich, et al., Phys. Rev. B 67 (2003) 094203.
- [5] R. Shuker, R. Gammon, Phys. Rev. Lett. 25 (1970) 222.
- [6] J. Jäckle, in: W.A. Phillips (Ed.), Amorphous Solids: Low-Temperature Properties, Springer, Heidelberg, 1981, p. 135.
- [7] J.S. Lannin, Phys. Rev. B 15 (1977) 3863; E. Duval, et al., J. Phys. Condens. Matter 2 (1990) 10227; P. Benassi, et al., Phys. Rev. B 44 (1991) 11734; M.G. Zemlyanov, et al., Sov. Phys. JETP 74 (1991) 151; T. Archibat, et al., J. Chem. Phys. 99 (1993) 2046; A.P. Sokolov, et al., Phys. Rev. B 48 (1993) 7692; E. Duval, et al., Phys. Rev. 48 (1993) 16785; T. Ohsaka, et al., Phys. Rev. 50 (1994) 9569; N.V. Surovtsev, et al., Phys. Rev. Lett. 82 (1999) 4476; V.N. Novikov, N.V. Surovtsev, Phys. Rev. B 59 (1999) 38; L. Saviot, et al., Phys. Rev. B 60 (1999) 18; E. Duval, et al., Philos. Mag. B 79 (1999) 11; B. Hehlen, et al., Phys. Rev. Lett. 84 (2000) 5355; N.V. Surovtsev, Phys. Rev. B 64 (2001) 061102; M. Ivanda, et al., Solid State Commun. 117 (2001) 423; N.V. Surovtsev, A.P. Sokolov, Phys. Rev. B 66 (2002) 054205; N.V. Surovtsev, et al., Phys. Rev. B 67 (2003) 024203; J. Phys. Condens. Matter 16 N.V. Surovtsev, N.V. Surovtsev, Phys. Status Solidi C 1 (2004) 2867; E. Courtens, et al., J. Phys. Condens. Matter 15 (2003) S1279; S.N. Yannopoulos, K.S. Andrikopoulos, J. Chem. Phys. 121 (2004) 4747; V.K. Malinovsky, et al., Europhys. Lett. 11 (1990) 43; N.J. Tao, G. Li, X. Chen, W.M. Du, H.Z. Cummins, Phys. Rev. A 44 (1991) 6665; A. Fontana, F. Rossi, G. Viliani, S. Caponi, E. Fabiani, G. Baldi, G. Ruocco, R. Dal Maschio, J. Phys. Condens. Matter 19 (2007) 205145; N.V. Surovtsev, S.V. Adichtchev, E. Rössler, M.A. Ramos, J. Phys. Condens. Matter 16 (2004) 223.
- [8] S.N. Yannopoulos, G.N. Papatheodorou, Phys. Rev. B 62 (2000) 3728; S.N. Yannopoulos, D.Th. Kastriosis, Phys. Rev. E 65 (2002) 021510.
- [9] B. Schmid, W. Schirmacher, Phys. Rev. Lett. 100 (2008) 137402.
- [10] T. Unruh, J. Neuhaus, W. Petry, Nucl. Instrum. Methods A 580 (2007) 1414.
- [11] W. Schirmacher, Europhys. Lett. 73 (2006) 892.
- [12] W. Schirmacher, et al., Phys. Rev. Lett. 98 (2007) 025501.
- [13] W. Schirmacher, et al., Phys. Stat. Sol. (c) 5 (2008) 862.

- [14] Y. Guo, S. Nonnenmann, A. Schulte, C. Rivero, K. Richardson, R. Stegeman, G. Stegeman, T. Cardinal, Conference on Lasers and Electro-Optics Technical Digest (OSA), CThP2, 2004.
- [15] L.D. Landau, E.M. Lifshitz, *Electrodynamics of Continuous Media*, Pergamon, New York, 1960, p. 391.
- [16] A.J. Martin, W. Brenig, *Phys. Status Solidi B* 64 (1974) 164.
- [17] U. Buchenau, *Z. Phys. B* 58 (1985) 181.
- [18] A. Schulte, Y. Guo, W. Schirmacher, T. Unruh, T. Cardinal, *Vib. Spectrosc.* 48 (2008) 12.